SEISMIC ACTIVE EARTH PRESSURE ON RIGID RETAINING WALLS UNDER ROTATION ABOUT BASE CONSIDERING PRINCIPAL-STRESS ROTATIONS BY PSEUDO-STATIC METHODS

SEIZMIČNI AKTIVNI ZEMELJSKI PRITISK NA TOGE PODPORNE STENE OB ROTACIJI OKOLI OSNOVE OB UPOŠTEVANJU ROTACIJE GLAVNE NAPETOSTI S PSEVDO-STATIČNO METODO

Yan-Yan Cai
Fujian Research Center for Tunneling and Urban Underground Space Engineering, Huaqiao University, No. 668 Jimei Road, Xiamen 361021, China
State Key Laboratory of Geohazard Prevention and Geoenvironment Protection, Chengdu University of Technology, No.1 Erxianqiao Road, Chengdu 610059, China
E-mail: yycai@hqu.edu.cn

Yi-Tao Zhou *(corresponding author)*
Hebei University of Water Resources and Electric Engineering, School of Civil Engineering
No.1 Chongqing Road, Cangzhou 061001, China
E-mail: zhouytwr@163.com

Wen-Ping Zhang
Huaqiao University,
School of Civil Engineering
No. 668 Jimei Road., Xiamen 361021, China
E-mail: zhangwxwz@163.com

Xiao-Yan Zhang
China University of Mining and Technology,
School of Mechanics and Civil Engineering
Ding No. 11 Xueyuan Road, Beijing 100083, China
E-mail: 899210@qq.com

Jin Yu
Huaqiao University,
School of Civil Engineering
No. 668 Jimei Road, Xiamen 361021, China
E-mail: bugyu0717@163.com

DOI https://doi.org/10.18690/actageotechslov.16.2.12-24.2019

Keywords

principal stress rotation; rigid retaining wall; rotation about base; seismic active earth pressure; seismic active rupture angle; pseudo-static method

Abstract

In this paper, new formulae for seismic active pressure on rigid retaining walls under the rotation about bases (RB) are derived by the pseudo–static method with the consideration of the principal stresses rotation. The calculation of seismic active earth pressure by pseudo-static method is transforming into that of static active earth pressure by the rotating calculation model. The seismic active rupture angle is obtained by Coulomb earth pressure theory. According to Mohr stress circle and the assuming the circular arc trajectory of minor principal stresses as a circular arch, the coefficient of the lateral seismic active earth

Ključne besede

rotacija glavne napetosti, toga podporna stena; vrtenje okoli osnove, seizmični aktivni zemeljski tlak, seizmični aktivni kot razpoke, psevdo-statična metoda

Izvleček

V tem prispevku so podane nove enačbe za izračun seizmičnega aktivnega tlaka na toge podporne zidove ob rotaciji okoli osnove (RB), izvedene s psevdo-statično metodo ob upoštevanju rotacije glavnih napetosti. Izračun seizmičnega aktivnega zemeljskega pritiska s psevdo-statično metodo je preoblikovan v statični aktivni zemeljski tlak z rotacijskim računskim modelom. Kot potresne aktivne razpoke dobimo s teorijo Coulombovega zemeljskega pritiska. Na osnovi Mohrove krožnice napetosti in ob predpostavki, da je trajektorija manjših glavnih napetosti krožni lok, sta, ob rotaciji okoli osnove, predlagana koefi-

pressure and the horizontal interfacial friction coefficient are proposed under RB mode. Then based on the force equilibrium of the differential sliding backfill element, the formula for the seismic active earth pressure on the rigid retaining wall under RB mode is obtained, as well as the formulae for the resultant of the seismic active earth pressure and the height of its application. Meanwhile, the effects of influence parameters on the seismic active rupture angle, the lateral seismic active earth pressure and its coefficient, the horizontal interfacial friction coefficient, the resultant of the seismic active earth pressure and the height of its application are discussed. Moreover, the comparisons of predicted values by the proposed method and M-O method are carried out as well as model tests. The result shows that the proposed method is more reasonable and effective than the M-O method.

cient bočnega seizmičnega aktivnega zemeljskega tlaka in medploskovni horizontalni koeficient trenja. S pomočjo ravnotežja sil diferenčnega drsnega zalednega elementa dobimo enačbo za seizmični aktivni zemeljski tlak, delujoč na togo podporno steno, ob rotaciji okoli osnove, kot tudi enačbi za rezultanto seizmičnega aktivnega zemeljskega tlaka in njeno ročico delovanja. V nadaljevanju obravnavamo vplive parametrov na seizmični aktivni kot razpoke, bočni seizmični aktivni zemeljski tlak in njegov koeficient, medploskovni horizontalni koeficient trenja, rezultanto seizmičnih aktivnih zemeljskih tlakov in njeno ročico delovanja. Poleg tega so izvedene primerjave napovedanih vrednosti po predlagani metodi z vrednostmi po metodi M-O ter modelnimi preizkusi. Rezultat kaže, da je predlagana metoda primernejša in bolj učinkovita kot metoda M-O.

1 INTRODUCTION

Retaining walls as a common retaining structure are widely used in geotechnical engineering of building foundations, highways, railways, riverbanks, etc. The distribution of the earth pressure is an important parameter in the design of retaining walls, and it is also the most fundamental and important problem in geotechnical engineering. For the frequent earthquake in the world scope, the analyses of various architectural structures under earthquake have been gradually becoming a hot subject. So, it is very necessary to consider the effects of seismic on earth pressures for the design of retaining structures. The pseudo-static and pseudo-dynamic methods are popularly used to calculate the seismic earth pressure. However, the pseudo-static method, which is first extended from Coulomb earth pressure theory, is more favored than the pseudo-dynamic method.

The most popular method of estimation the active earth pressure during earthquakes is the M-O method. Okabe [1] and Mononobe & Matsuo [2] firstly extended the Coulomb theory to seismic earth pressures by the pseudo-static method. The distribution of the seismic earth pressure on a rigid retaining wall by M-O method is linear along the wall height. However, some experiments [3, 4, 5] have shown that this distribution is nonlinear. In recent decades, many researchers improved the calculation of the seismic earth pressure by the pseudo–static method [6-13] and the pseudo–dynamic theory [14-17]. Based on the limit equilibrium theory, Azad et al. [18] applied the pseudo-dynamic method into the horizontal slice method of analysis with the consideration of the effect of earthquake on the lateral earth pressure. Utilizing a composite logarithmic spiral failure surface at which the Mohr-Coulomb failure criterion is enforced and a limit-equilibrium approach, a slice method for estimating seismic earth pressures based on the pseudo-static method was put forward by Shamsabadi et al. [19]. Chen et al. [20] used the limit equilibrium variational method to study the seismic active earth pressure under general conditions. For the friction stress on the wall, the directions of the major and minor principal stresses are rotated. So, some researchers [21-27] took into account the effect of the principal-stress rotation on static active earth pressures for translating rigid retaining walls, and Li et al. [27] took into account this effect on static active earth pressures for rigid retaining walls under the rotation about bases. And other researchers [12,13, 17] considered the effect of principal-stress rotations on seismic active and passive earth pressures for the translating retaining wall by the pseudo-static and pseudo-dynamic methods. But in these studies of seismic active earth pressures, the rotation of principal stresses which is a well-established phenomenon in geotechnical engineering is seldom considered.

In this paper, by rotating the pseudo-static calculation model for seismic active earth pressure under earthquakes, the seismic active rupture angle is derived according to Coulomb static earth pressure theory. Then, according to the Mohr stress circle, stresses of the backfill behind the rigid retaining wall under the earthquake are were obtained. And by assuming the trajectory of the minor principal stress as a circular arc, the coefficient of the lateral seismic active earth pressure under RB mode and the horizontal interfacial friction coefficient is proposed by integrating shear stress and vertical stress on the horizontal in the sliding backfill. Furthermore, by force equilibrium of the differential sliding backfill element, analytical solutions for the seismic active earth pressure are obtained. In addition, to check the accuracy of the proposed solutions, comparisons of seismic active earth pressures by the proposed method and M-O method are carried out with the experimental results. Furthermore, parametric studies are investigated.

2 PSEUDO-STATIC ANALYSIS OF THE SEISMIS LOAD

The pseudo-static method is generally applied to the calculation of the seismic earth pressure. The horizontal and vertical inertia forces F_h and F_v of the backfill under the seismic load are calculated by the pseudo-static method as follows:

$$F_h = k_h \rho g \qquad (1)$$

$$F_v = (1-k_v)\rho g \qquad (2)$$

where k_h is the horizontal seismic coefficient; k_v is the vertical seismic coefficient; ρ is the density of soil; g is the gravitational acceleration.

According to Fig.1, the seismic angle between the direction of the total acceleration and the plumb line is obtained as follows:

$$\eta = \arctan\frac{F_h}{F_v} = \arctan\frac{k_h \rho g}{(1-k_v)\rho g} = \arctan\frac{k_h}{1-k_v} \qquad (3)$$

Then the total inertia force composed of the gravity and the seismic force can be calculated as follows:

$$F = \frac{(1-k_v)\rho g}{\cos\eta} \qquad (4)$$

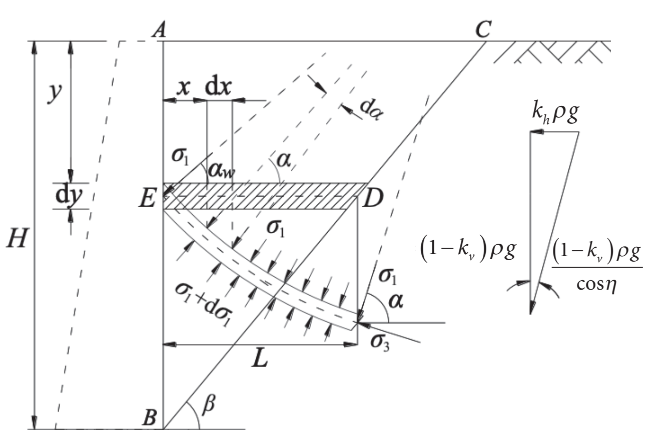

Figure 1. Principal stresses of sliding backfill under seismic load.

3 THEORETICAL ANALYSIS

A vertical rigid retaining wall with height H is analyzed with a cohesionless backfills as shown in Fig. 1. The unit weight of backfills is γ, the wall-soil friction angle is δ, the friction angle of backfills is φ, and the horizontal and vertical seismic accelerations are respectively $k_h g$ and $k_v g$. A sliding surface exists in the backfill behind the rigid retaining wall under the limit equilibrium state, which is approximates to a plane at an angle of β to the horizontal.

3.1 Seismic active rupture angle

To obtain the seismic active rupture angle by Coulomb static earth pressure, rotating the original model calculated seismic earth pressures shown in Fig. 1 with the counterclockwise angle η yields a new inclined rigid retaining wall as shown in Fig. 2. Then the seismic active earth pressure on the vertical rigid retaining wall by pseudo-static mothed is equal to the static active earth pressure on the rigid retaining wall with an inclined angle of η, a height of $H' = H\cos\eta$ and an unit weight of $\gamma' = \gamma(1-k_v)/\cos\eta$. According to Coulomb static earth pressure theory, the seismic active earth pressure can be obtained by analyzing the static active earth pressure on this inclined rigid retaining wall as shown in Fig.2:

$$E = \frac{(1-k_v)\gamma H^2 \cos(\beta'-\eta)\sin(\beta'-\varphi)}{2\cos\eta\sin(\beta'-\eta)\cos(\beta'-\varphi-\delta-\eta)} \qquad (5)$$

$$\beta' = \beta + \eta \qquad (6)$$

where β' is the pseudo-static seismic active rupture angle.

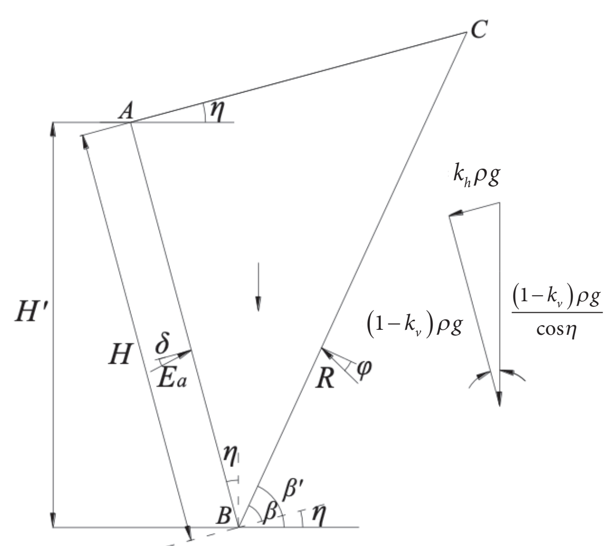

Figure 2. The calculation model of seismic active rupture angle.

From Eqs. (5 and 6), solving $\mathrm{d}E/\mathrm{d}\beta' = 0$ yields the seismic active rupture angle:

$$\beta = \beta' - \eta = \arctan\left\{\tan(\varphi-\eta)\left[1+\sqrt{1+\cot(\varphi+\delta)\cot(\varphi-\eta)}\right]\right\} \tag{7}$$

3.2 Stresses of the differential sliding backfill element

The relationship between the stresses and the principal stresses at any point of the horizontal in the differential sliding backfill element can be expressed by the Mohr stress circle as shown in Fig.3(a), and the stresses of the backfill at the wall surface and sliding surface are respectively shown as Fig.3(b) and Fig.3(c).

From Fig.3(a), the lateral and vertical earth stresses at any point of a distance x from the wall and a depth y from the backfill surface can be obtained as follows:

$$\sigma_h = \sigma_1 \cos^2\alpha + \sigma_3 \sin^2\alpha \tag{8}$$

$$\sigma_v = \sigma_1 \sin^2\alpha + \sigma_3 \cos^2\alpha \tag{9}$$

where α is the rotational angle of principal stresses at any point in sliding backfills; σ_1 and σ_3 are the major and minor principal stresses, respectively.

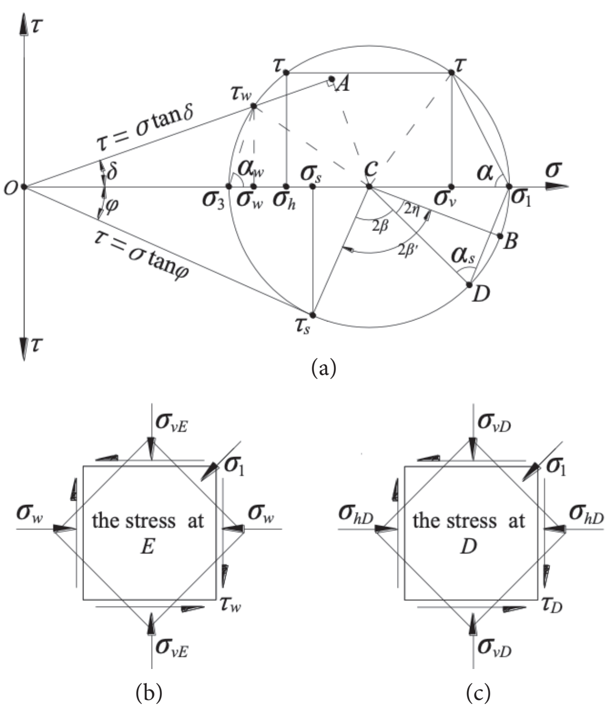

Figure 3. Stresses of sliding backfill (a) Mohr stress circle. (b) The stresses of the backfill at the wall surface. (c) The stresses of the backfill at the sliding surface.

The shear stress at any point of a distance x from the wall and a depth y from the backfill surface can be calculated as follows:

$$\tau = \frac{\sigma_1 - \sigma_3}{2}\sin 2\alpha \tag{10}$$

Similarly, according to Fig.3(a), the lateral earth stress and shear stress on the wall at a depth y can be obtained as follows:

$$\sigma_w = \sigma_1 \cos^2\alpha_w + \sigma_3 \sin^2\alpha_w \tag{11}$$

$$\tau_w = \sigma_w \tan\delta \tag{12}$$

The shear stress and normal stress on the sliding surface at a depth y can be calculated as follows:

$$\tau_s = \frac{(\sigma_1 - \sigma_3)\cos\varphi}{2} \tag{13}$$

$$\sigma_s = \frac{\tau_s}{\tan\varphi} = \frac{(\sigma_1 - \sigma_3)\cos^2\varphi}{2\sin\varphi} \tag{14}$$

From the geometry knowledge in Fig.1, the rotational angle of the principal stress at the wall can be obtained from the equation:

$$\alpha_w = \frac{\pi}{4} + \frac{\delta}{2} + \frac{1}{2}\arccos\frac{\sin\delta}{\sin\varphi} \tag{15}$$

The angle of the minor principal stress plane to the sliding surface can be calculated as follows:

$$\alpha_\beta = \frac{\pi}{4} + \frac{\varphi}{2} \tag{16}$$

From the geometry knowledge in Fig.1, the rotational angle of the principal stress at the sliding surface can be obtained as follows:

$$\alpha_s = \frac{\pi}{2} - \alpha_\beta + \beta = \frac{\pi}{4} - \frac{\varphi}{2} + \beta = \frac{\pi}{4} - \frac{\varphi}{2} + \arctan\left\{\tan(\varphi-\eta)\left[1+\sqrt{1+\cot(\varphi+\delta)\cot(\varphi-\eta)}\right]\right\} \tag{17}$$

3.3 Seismic active stress coefficients

The trajectory of the principal stresses has been observed or inferred to be elliptic, catenary [23, 28], circular arc [29-32] and parabolic [22, 25]. In this study, it is assumed that the trajectory of the minor principal stresses is a circular arc as shown in Fig.1. According to Fig.1, the following expressions can be obtained:

$$\mathrm{d}x = R\sin\alpha\,\mathrm{d}\alpha \tag{18}$$

$$\alpha = \arccos\left(\cos\alpha_w - \frac{x}{R}\right) \tag{19}$$

The horizontal width L of the differential sliding backfill element at a depth y from the backfill surface can be calculated as follows:

$$L = R(\cos\alpha_w - \cos\alpha_s) \quad (20)$$

The gravity of the differential sliding backfill element is obtained as follows:

$$dG = \gamma(H-y)\cot\beta dy \quad (21)$$

The average vertical stress σ_{av} and the average shear stress τ_a on the horizontal of the sliding backfill at a depth y can be respectively calculated as follows:

$$\begin{aligned}\sigma_{av} &= \frac{\int_0^L \sigma_v dx}{L} = \frac{\int_{\alpha_w}^{\alpha_s} \sigma_1(\sin^2\alpha + k_a\cos^2\alpha)R\sin\alpha d\alpha}{L} \\ &= \sigma_1\left[1 - \frac{1-k_a}{3}(\cos^2\alpha_s + \cos\alpha_w\cos\alpha_s + \cos^2\alpha_w)\right]\end{aligned} \quad (22)$$

$$\begin{aligned}\tau_a &= \frac{\int_0^L \tau dx}{L} = \frac{\int_{\alpha_w}^{\alpha_s} \frac{1-k_a}{2}\sigma_1 \sin 2\alpha R\sin\alpha d\alpha}{L} \\ &= \frac{\sigma_1(1-k_a)(\sin^3\alpha_s - \sin^3\alpha_w)}{3(\cos\alpha_w - \cos\alpha_s)}\end{aligned} \quad (23)$$

where

$$k_a = \frac{\sigma_3}{\sigma_1} = \frac{1-\sin\varphi}{1+\sin\varphi} \quad (24)$$

Dividing Eq. (11) by Eq. (22) yields the coefficient of the lateral seismic active earth pressure under RB mode:

$$k_{aw} = \frac{\sigma_w}{\sigma_{av}} = \frac{\cos^2\alpha_w + k_a\sin^2\alpha_w}{1 - \frac{1-k_a}{3}(\cos^2\alpha_s + \cos\alpha_w\cos\alpha_s + \cos^2\alpha_w)} \quad (25)$$

From Eq. (25), the coefficient of the lateral seismic active earth pressure k_{aw} is similar to the coefficient of the lateral static active earth pressure calculated by Rao et al. [30], but the α_s in the two coefficients are different.

Dividing Eq. (23) by Eq. (22) gives the horizontal interfacial friction coefficient under RB mode:

$$\tan\varphi' = \frac{\tau_a}{\sigma_{av}} = \frac{(1-k_a)(\sin^3\alpha_s - \sin^3\alpha_w)}{3(\cos\alpha_w - \cos\alpha_s) - (1-k_a)(\cos^3\alpha_w - \cos^3\alpha_s)} \quad (26)$$

where φ' is the horizontal interfacial friction angle.

3.4 Seismic active earth pressure

The analytic model of the differential sliding backfill element behind the rigid retaining wall under RB mode is shown in Fig. 4.

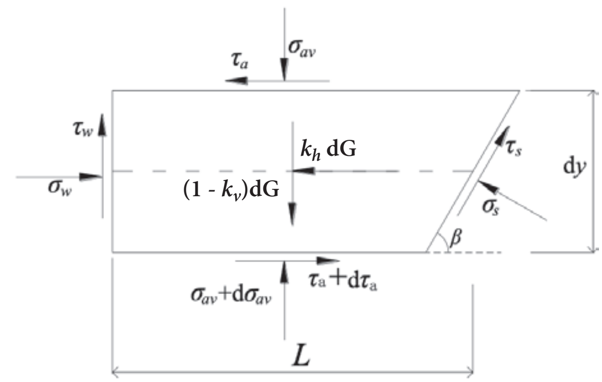

Figure 4. Stresses on differential sliding backfill element.

Analyzing the horizontal and vertical force equilibrium of the differential sliding backfill element yield the following equations:

$$\begin{aligned}&\sigma_w + \tau_s\cot\beta + (H-y)\frac{d\tau_a}{dy}\cot\beta \\ &\quad - k_h\gamma(H-y)\cot\beta - \sigma_s - \tau_a\cot\beta = 0\end{aligned} \quad (27)$$

$$\begin{aligned}&\tau_w + (H-y)\frac{d\sigma_{av}}{dy}\cot\beta + \tau_s + \sigma_s\cot\beta \\ &\quad - (1-k_v)\gamma(H-y)\cot\beta - \sigma_{av}\cot\beta = 0\end{aligned} \quad (28)$$

where dy is the thickness of the differential sliding backfill element.

By Eqs. (12, 14, 25 and 26), the following expressions can be got:

$$\begin{aligned}\tau_w &= \sigma_w\tan\delta \qquad & \tau_s &= \sigma_s\tan\varphi \\ \sigma_w &= k_{aw}\sigma_{av} \qquad & \tau_a &= \sigma_{av}\tan\varphi'\end{aligned} \quad (29)$$

From Eqs. (27 and 29), the differential equation of the average vertical stress can be obtained as follows:

$$\frac{d\sigma_{av}}{dy} = \frac{1-A}{H-y}\sigma_{av} + B\gamma \quad (30)$$

where

$$A = k_{aw}\tan\beta\frac{1+\tan(\beta-\varphi)\tan\delta}{\tan(\beta-\varphi)+\tan\varphi'} \quad (31)$$

$$B = \frac{\cos\varphi'}{\sin(\beta-\varphi+\varphi')}\left[(1-k_v)\sin(\beta-\varphi) + k_h\cos(\beta-\varphi)\right] \quad (32)$$

Integrating Eq. (30) yields the average vertical stress as follows:

$$\sigma_{av} = \frac{\gamma B(H-y)}{A-2} + C(H-y)^{(A-1)} \qquad (33)$$

where C is the integration constant.

By the boundary conditions $\sigma_{av} = 0$ at $y = 0$, substituting $\sigma_{av} = 0$ and $y = 0$ into Eq. (33) gives C as follows:

$$C = \frac{B\gamma}{2-A} H^{(2-A)} \qquad (34)$$

Substituting Eq. (34) into Eq. (33) yields the average vertical stress:

$$\sigma_{av} = \frac{\gamma HB}{A-2}\left[\frac{H-y}{H} - \left(\frac{H-y}{H}\right)^{(A-1)}\right] \qquad (35)$$

From Eqs. (29 and 35), the lateral seismic active earth pressure can be obtained:

$$\sigma_w = k_{aw}\sigma_{av} = k_{aw}\frac{\gamma HB}{A-2}\left[\frac{H-y}{H} - \left(\frac{H-y}{H}\right)^{(A-1)}\right] \qquad (36)$$

Integrating Eq. (36) yields the resultant of the lateral seismic active earth pressure:

$$E_h = \int_0^H \sigma_w \mathrm{d}y = k_{aw}\frac{\gamma H^2}{2}\frac{B}{A} \qquad (37)$$

From Eq. (37), the resultant of the seismic active earth pressure can be calculated:

$$E_a = \frac{E_h}{\cos\delta} = \frac{k_{aw}}{\cos\delta}\frac{\gamma H^2}{2}\frac{B}{A} \qquad (38)$$

Substituting Eqs. (31 and 32) into Eq. (38) yields:

$$E_a = \frac{(1-k_v)\gamma H^2 \sin(\beta+\eta-\varphi)}{2\cos\eta\tan\beta\cos(\beta-\varphi-\delta)} \qquad (39)$$

Substituting Eq. (6) into Eq. (5) also yields Eq. (39), this verifies it is correct that the derivation of the seismic active earth pressure under RB mode considering principal stress rotation by pseudo-static method.

From Eq. (36), the moment M of the resultant of the lateral seismic active earth pressure about the wall base is obtained by integrating $\sigma_w(H-y)$ with respect to y as follows:

$$M = \int_0^H \sigma_w (H-y)\mathrm{d}y = k_{aw}\frac{\gamma H^3 B}{3(A+1)} \qquad (40)$$

Dividing Eq. (40) by Eq. (37) gives the height of the application of the E_h:

$$h = \frac{M}{E_h} = \frac{H}{3}\frac{2A}{A+1} \qquad (41)$$

Letting $A = 1$ in Eq. (41), the height of the application of the seismic active earth pressure is equal to that of the static active earth pressure obtained by Rankine and Coulomb.

4 COMPARISONS

To check the applicability of the proposed method, the calculated values of the lateral seismic active earth pressure under RB mode by Eq. (36) are compared with those by M-O method and the experimental results under RB mode by Ishibashi and Fang [4], as shown in Fig. 5. The parameters considered in the field test by Ishibashi and Fang [4] were: $\varphi = 40°$, $\delta = 20°$, $k_h = 0.215$ and $k_v = 0$.

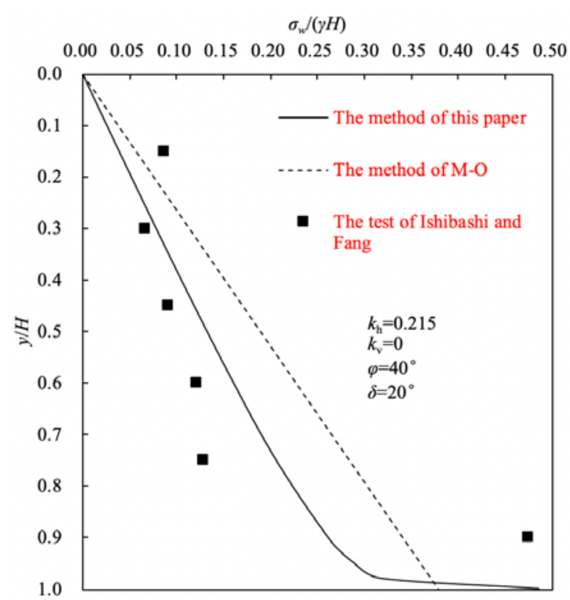

Figure 5. Comparison of the lateral seismic active earth pressure.

It can be seen clearly from Fig. 5 that the distributions of the lateral seismic active earth pressure by the proposed method and by field test are non-linear, but this distribution by M-O method is linear. This is because in the M-O method the distribution of the lateral seismic active earth pressure was assumed to be linear, and the displacement mode of the retaining wall and the principal-stresses rotation were not considered. Fig. 5 shows that the results obtained by the proposed method is closer to the measured values than those by M-O method. Therefore, it is proved that the seismic active earth pressure predicted by the proposed method is feasible and reasonable for the design of retaining walls under RB mode.

5 PARAMETRIC STUDY

5.1 Seismic active rupture angle

Figs. 6 and 7 show the variations of the seismic active rupture angle β under RB mode with the horizontal and vertical seismic coefficients, internal friction angle of backfills and wall–soil friction angle.

Figs. 6 and 7 show that the seismic active rupture angles β are always smaller than $\pi/4+\varphi/2$. The β increases with the increase of φ, but it decreases with the increase of k_h and k_v respectively, and it almost decreases linearly with the increase of δ. Moreover, the effect of φ on β is greater than that of δ.

5.2 Coefficient of lateral seismic active earth pressure

Figs. 8-11 show the variations of the coefficient k_{aw} of the lateral seismic active earth pressure under RB mode with the horizontal and vertical seismic coefficients, internal friction angle of backfills and wall–soil friction angle.

From Figs. 8-11, the k_{aw} is smaller than 0.5, and non-linearly decreases with the increase of φ. But k_{aw} non-linearly increases with the increases of δ, k_h and k_v, respectively.

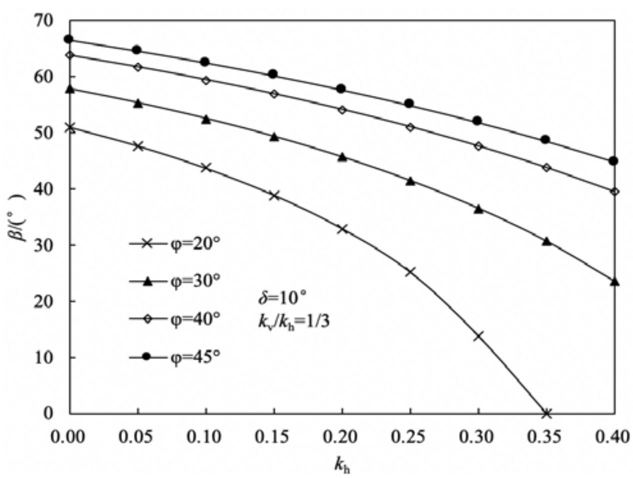

Figure 6. Effect of the horizontal seismic coefficient on β under different φ.

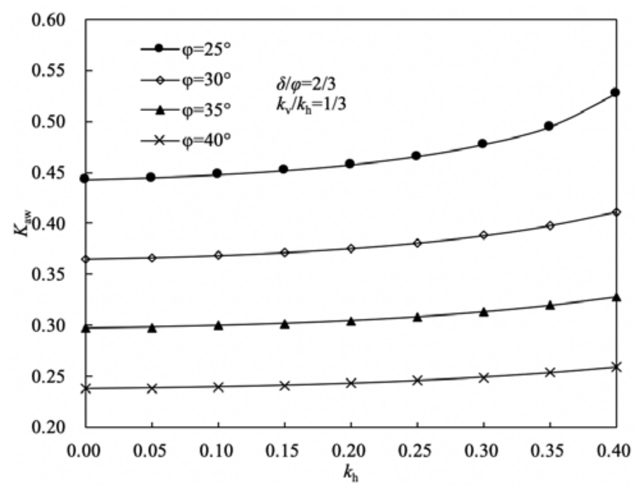

Figure 8. Effect of the horizontal seismic coefficient on k_{aw} under different φ.

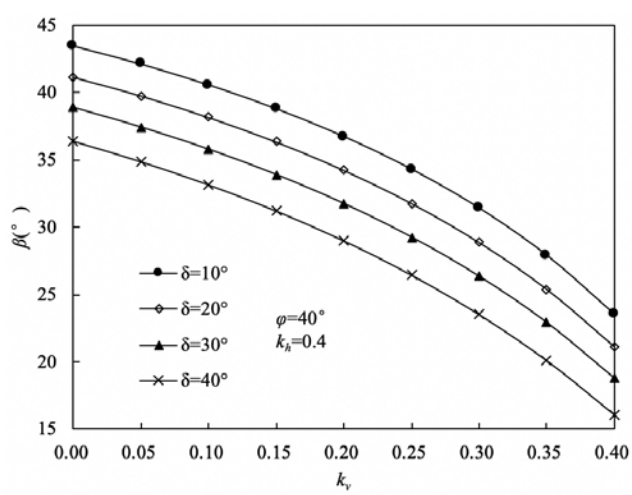

Figure 7. Effect of the vertical seismic coefficient on β under different δ.

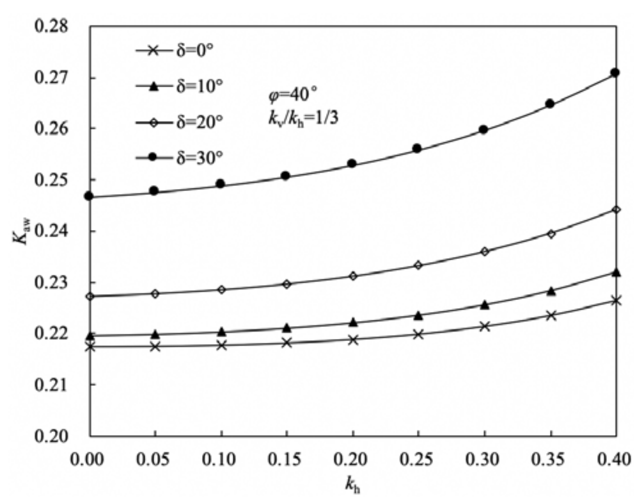

Figure 9. Effect of the horizontal seismic coefficient on k_{aw} under different δ.

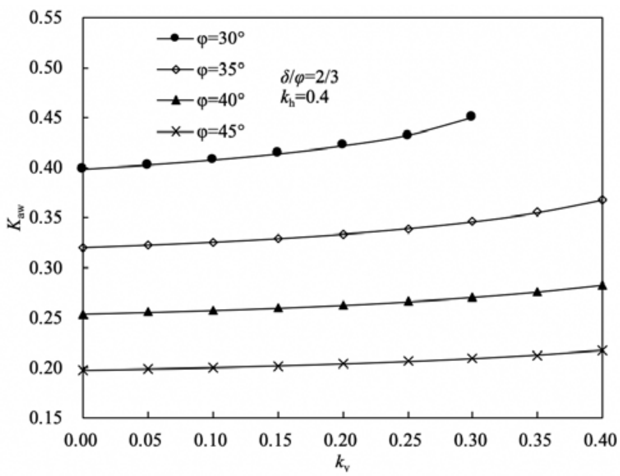

Figure 10. Effect of the vertical seismic coefficient on k_{aw} under different φ.

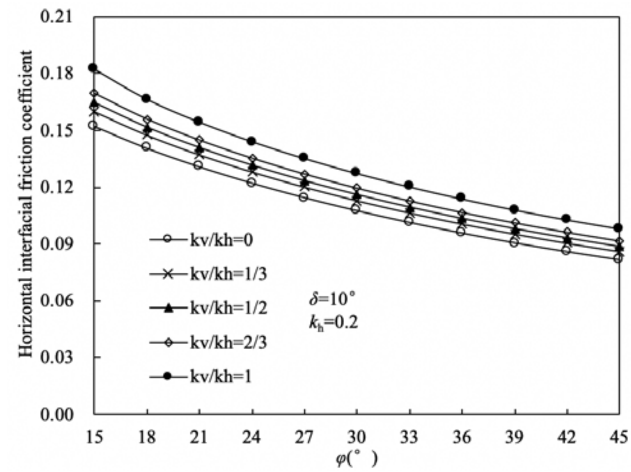

Figure 12. Effects of the internal friction angle on tanφ' under different k_v/k_h.

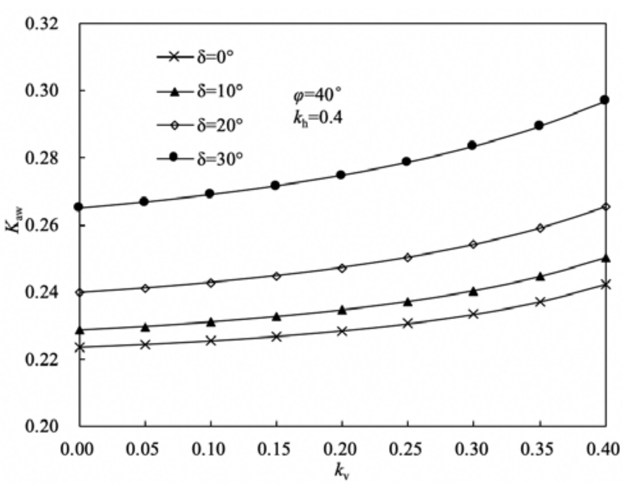

Figure 11. Effect of the vertical seismic coefficient on k_{aw} under different δ.

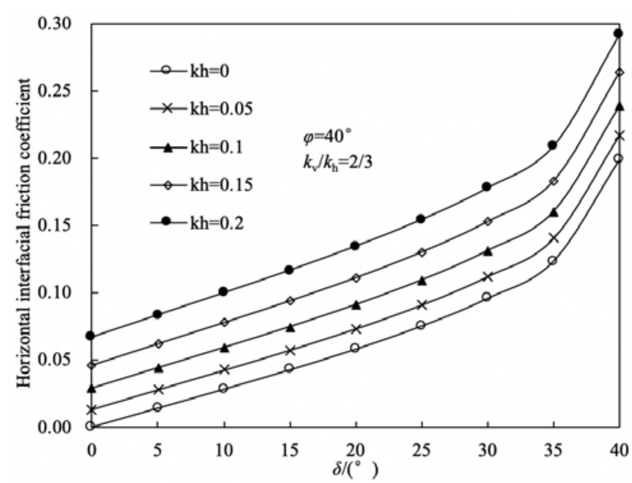

Figure 13. Effects of the wall–soil friction angle on tanφ' under different k_h.

5.3 Horizontal interlayer friction coefficient

Figs. 12 and 13 show the variations of the horizontal interfacial friction coefficient with these influence parameters (i.e. the internal friction angle φ, horizontal seismic coefficient k_h and vertical seismic coefficient k_v).

From Fig. 12, the horizontal interlayer friction coefficient tanφ' decreases from 0.18 to 0.09 with the increase of φ from 15° to 45° and with the decrease of k_v from 0 to k_h. From Fig. 13, the tanφ' increase from 0 to 0.3 with the increase of δ from 0 to φ and k_h from 0 to 0.2, and it is smaller than tanφ = tan40° = 0.839. Moreover from Fig. 12 and Fig. 13, it can be seen obviously that influence of k_h on tanφ' is more significant than that of k_v on tanφ', and the influence of δ on tanφ' is more significant than that of φ on tanφ'.

5.4 Lateral seismic active earth pressure

Figs. 14-17 show the distributions of the normalized lateral seismic active earth pressure $\sigma_w/(\gamma H)$ along the normalized wall height with φ, δ, k_h and k_v.

From Figs. 14-17, the maximum value of the lateral seismic active earth pressure is located near the wall toe,that is consistent with the experimental results [4] for rigid retaining walls under RB mode. Moreover, the lateral seismic active earth pressure σ_w is concave nonlinear distribution along the wall height except for k_h<0.1, and the distribution of σ_w varies from right-convex to concave with increase of k_h from 0 to 0.2. The σ_w decreases with the increase of φ, δ and k_v, respectively. But the σ_w increases with the increase of k_h.

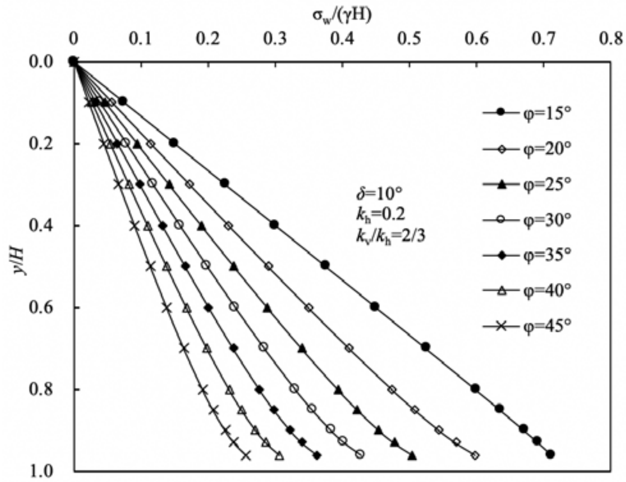

Figure 14. Effect of the internal friction angle on $\sigma_w/(\gamma H)$.

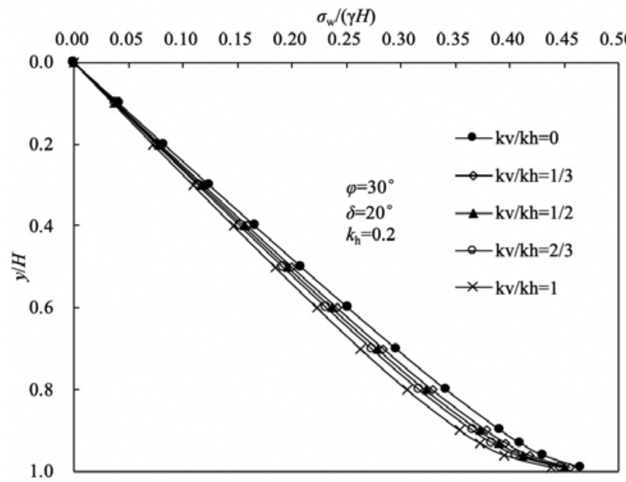

Figure 17. Effect of the ratio between the vertical and horizontal seismic coefficients on $\sigma_w/(\gamma H)$.

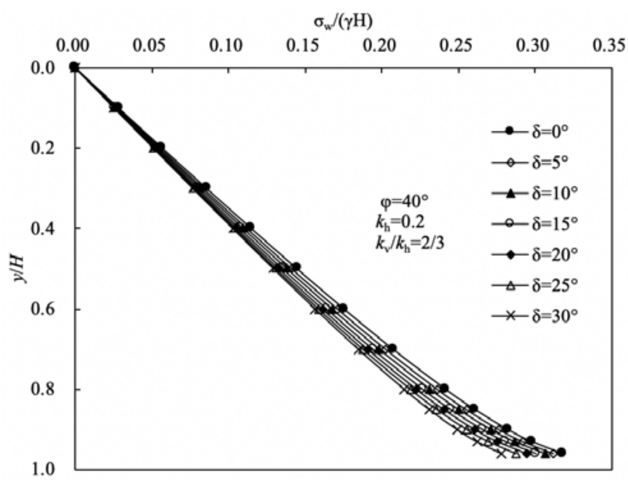

Figure 15. Effect of the wall–soil friction angle on $\sigma_w/(\gamma H)$.

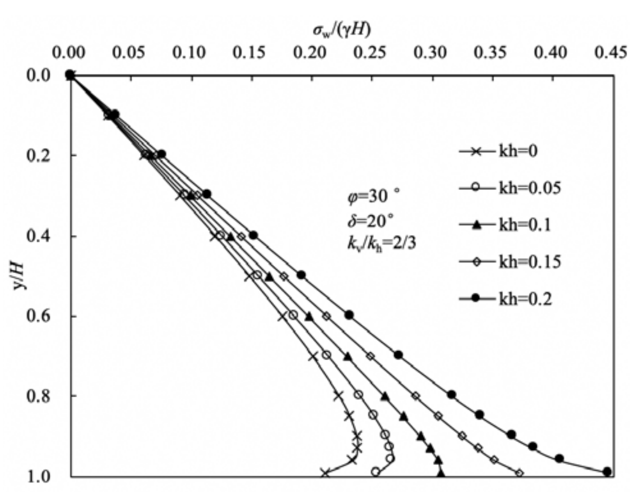

Figure 16. Effect of the horizontal seismic coefficient on $\sigma_w/(\gamma H)$.

From Figs. 14-17, the resultant of the seismic active earth pressure respectively decreases with the increase ofφ, δ and k_v, but increases with the increase of k_h.

5.5 Height of the application of the seismic active earth pressure

Figs. 18-19 show the variations of the normalized height of the application of the seismic active earth pressure h/H with φ, δ/φ, k_h and k_v/k_h.

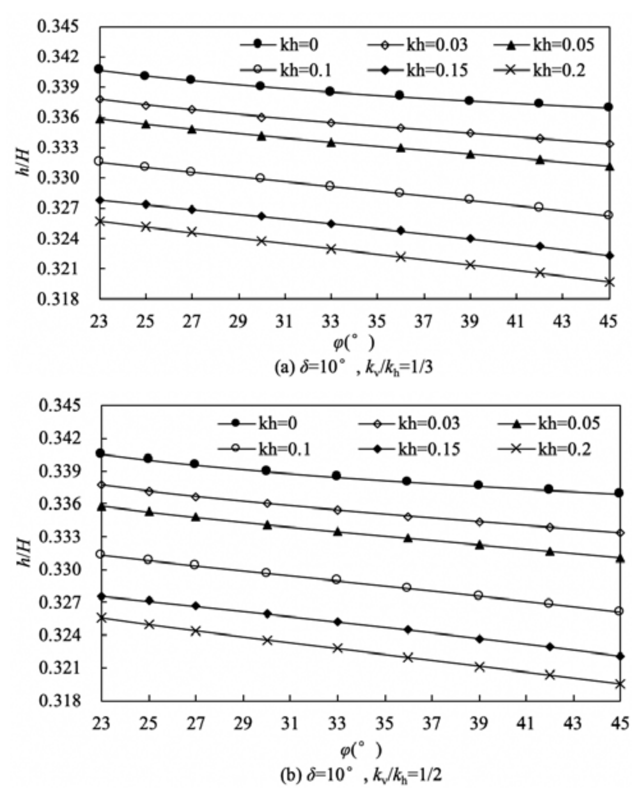

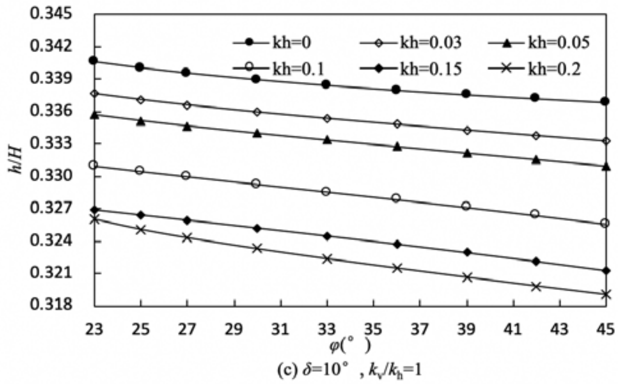

Figure 18. Change of the height of the application of the lateral seismic active earth pressure with φ under different k_h.

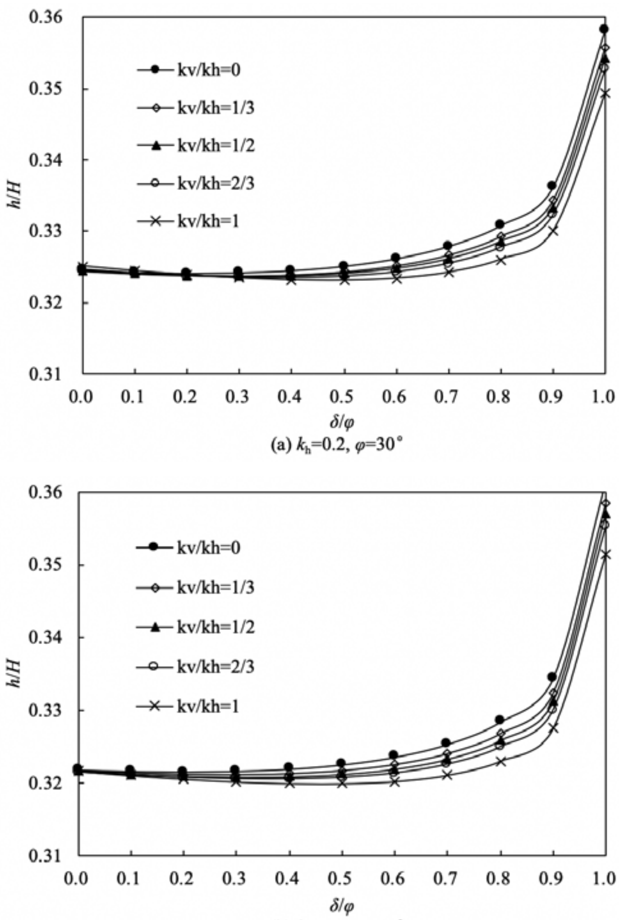

Figure 19. Change of the height of the application of the lateral seismic active earth pressure with δ/φ under different k_v/k_h.

From Figs. 18 and 19, the normalized height of the application of the lateral seismic active earth pressure h/H approximately decreases linearly with the increase of φ, and first decreases and then increases with the increase of δ/φ, but it non-linearly decreases with the increase of k_h. Moreover, the h/H increases with the increase of k_v/k_h for $\delta/\varphi \le 0.1$ and $\varphi \le 28°$, but decreases with the increase of k_v/k_h for $\delta/\varphi \ge 0.6$.

The h/H is greater than 1/3 and smaller than 0.3406 for $k_h \le 0.03$, but it is smaller than 1/3 and greater than 0.319 for $k_h \ge 0.1$. Moreover, the h/H is smaller than 1/3 and greater than 0.3311 for $\varphi > 33°$ and $k_h = 0.05$, and it is smaller than 1/3 and greater 0.3199 for $\delta/\varphi \le 0.8$ and $k_h > 0$, but it is greater than 1/3 and smaller than 0.3359 for $23° \le \varphi \le 33°$ and $k_h = 0.05$.

6 CONCLUSIONS

In the proposed method, the seismic problem was simplified to the static problem using the pseudo-static method. By rotating, the seismic angle is added to the inclined angles of the wall and backfill surface in the formula of Coulomb static earth pressure, then the seismic active rupture angle was obtained according to Coulomb static earth pressure theory. Moreover, the basic equations of the seismic active earth pressure under RB mode were established by stress analysis and the static equilibrium. Then, the theoretical formulae for the seismic active earth pressure and its coefficient, the resultant of the seismic active earth pressure and its application height are put forward for the design of rigid retaining walls under RB mode considering the principal-stress rotation.

The effects of main parameters (i.e. the internal friction angle of backfills, wall-soil friction angle, horizontal and vertical seismic coefficients) on the seismic active rupture angle, the coefficient of the lateral seismic active earth pressure, the horizontal interface friction coefficient, the distribution of the seismic active earth pressure, the resultant earth pressure and the height of its application were analyzed. The horizontal seismic coefficient has a greater influence on the seismic active earth pressure of rigid retaining walls than the vertical seismic coefficient, and the internal friction angle of backfills has a greater influence on the seismic active earth pressure of rigid retaining walls than the wall-soil friction angle. The comparisons of predicted and measured values of the lateral seismic active earth pressure showed that the proposed method agreed better with the experiment than M-O method. This proposed method is feasible and reasonable in the design of seismic rigid retaining walls under RB mode.

Acknowledgments

This research was supported by the Natural Science Foundation of China (Grant 51774147 and 51978292), Natural Science Foundation of Fujian Province of China (Grants

2017J01669 and 2017J01094), Scientific Research Program of Hebei Education Department (Grant QN2018098) and Opening Fund of State Key Laboratory of Geohazard Prevention and Geoenvironment Protection (Chengdu University of Technology), China (SKLGP2018K008). All support is gratefully acknowledged.

Notation

The following symbols are used in this paper:

F_h = horizontal inertia force of the backfill
F_v = vertical inertia force of the backfill
F = total inertia force of the backfill
k_h = horizontal seismic coefficient
k_v = vertical seismic coefficient
ρ = density of the backfill
g = gravitational acceleration
k_hg = horizontal seismic acceleration
k_vg = vertical seismic acceleration
η = seismic angle
γ = unit weight of the backfill
γ' = unit weight of the backfill in rotating calculation model
δ = wall-soil friction angle
φ = internal friction angle of backfills
β = seismic active rupture angle
β' = pseudo seismic active rupture angle
H = height of the rigid retaining wall
H' = height of the rigid retaining wall after rotation
α = rotational angle of principal stresses
σ_1 = major principal stress
σ_3 = minor principal stress
σ_h = horizontal stress on the vertical of the differential sliding backfill element at any point
σ_v = vertical stress on the horizontal of the differential sliding backfill element at any point
τ = shear stress on horizontal of the differential sliding backfill element at any point
σ_w = lateral earth pressure on the wall
τ_w = shear stress on the wall
α_w = rotational angle of the principal stress at the wall
τ_s = shear stress on the sliding surface
σ_s = normal stress on the sliding surface
α_β = angle between the active sliding surface and the major principal stress plane
α_s = angle between the horizontal and major principal stress at the sliding surface
dx = differential length along the horizontal
L = horizontal width of the differential flat element
R = radius of the circular arc
x = horizontal distance of arbitrary point in differential flat element from the wall
y = depth of the differential element from the backfill surface
dG = self-weight of differential sliding backfill element
σ_{av} = average vertical stress on the horizontal in differential element
τ_a = average shear stress on the horizontal in differential element
k_a = coefficient of active earth pressure by Rankine
k_{aw} = coefficient of lateral seismic active earth pressure in this paper
φ' = horizontal interlayer friction angle
$\tan\varphi'$ = interfacial friction coefficient
E_h = resultant of lateral seismic active earth pressure on the retaining wall
E_a = resultant of seismic active earth pressure on the retaining wall
M = moment of the lateral seismic active earth pressure about the wall base
h = height of application of the seismic active earth pressure

REFERENCES

[1] Okabe, S. 1926. General theory of earth pressure. Journal of the Japanese society of Civil Engineers 12(1), 1277–1323.

[2] Mononobe, N., Matsuo, O. 1929. On the determination of earth pressure during earthquakes. Proceeding of the World Engineering Congress, 9, Tokyo, Japan, pp. 179–187.

[3] Khosravi, M.H., Pipatpongsa, T., Takemura, J. 2013. Experimental analysis of earth pressure against rigid retaining walls under translation mode. Géotechnique 63(12), 1020-1028. DOI: 10.1680/geot.12.P.021

[4] Ishibashi, I., Fang, Y.S. 1987. Dynamic earth pressures with different wall movement modes. Soils and Foundations 27(4), 11-22. DOI:10.3208/sandf1972.27.4-11

[5] Sherif, M.A., Fang, Y.S. 1984. Dynamic earth pressures on walls rotating about the top. Soils and Foundations 24(4), 109-117. DOI:10.3208/sandf1972.24.4-109

[6] Ghosh, S., Debnath, C. 2016. Pseudo-static analysis of reinforced earth retaining wall considering non-linear failure surface. Geotechnical and Geological Engineering 34(4), 981-990. DOI: 10.1007/s10706-016-0018-6

[7] Iskander, M., Chen, Z., Omidvar, M., Guzman, I., Elsherif, O. 2013. Active static and seismic earth pressure for c–φ, soils. Soils and Foundations 53, 639–652. DOI: 10.1016/j.sandf.2013.08.003

[8] Caltabiano, S., Cascone, E., Maugeri, M. 2012. Static and seismic limit equilibrium analysis of sliding retaining walls under different surcharge conditions. Soil Dynamics and Earthquake Engineering 37(6), 38-55. DOI: 10.1016/j.soildyn.2012.01.015

[9] Nouri, H., Fakher, A., Jones, C.J.F.P. 2008. Evaluating the effects of the magnitude and amplification of pseudo-static acceleration on reinforced soil slopes and walls using the limit equilibrium horizontal slices method. Geotextiles and Geomembranes 26(3), 263-278. DOI: 10.1016/j.geotexmem.2007.09.002

[10 Choudhury, D., Singh, S. 2006. New approach for estimation of static and seismic active earth pressure. Geotechnical and Geological Engineering 24(1), 117-127. DOI: 10.1007/s10706-004-2366-x

[11] Rao, K.S.S., Choudhury, D. 2005. Seismic passive earth pressures in soils. Journal of Geotechnical and Geoenvironmental Engineering 131(1), 131-135. DOI: 10.1061/(ASCE)1090-0241(2005)131:1(131)

[12] Zhou, Y., Chen, F. 2015. Seismic active earth pressure for non-vertical rigid retaining wall considering soil arching effect. Chinese Journal of Rock Mechanics & Engineering 34(7), 1452-1461. DOI:1000-6915(2015)07-1452-10 (In Chinese)

[13] Pain, A., Chen, Q., Nimbalkar, S., Zhou, Y. 2017. Evaluation of seismic passive earth pressure of inclined rigid retaining wall considering soil arching effect. Soil Dynamics & Earthquake Engineering 100(9), 286-295. DOI: 10.1016/j.soildyn.2017.06.011

[14] Choudhury, D., Katdare, A.D., Pain, A. 2014. New method to compute seismic active earth pressure on retaining wall considering seismic waves. Geotechnical and Geological Engineering 32(2), 391-402. DOI: 10.1007/s10706-013-9721-8

[15] Ghosh, S., Sharma, R.P. 2012. Seismic active earth pressure on the back of battered retaining wall supporting inclined backfill. International Journal of Geomechanics 12(1), 54-63. DOI: 10.1061/(ASCE)GM.1943-5622.0000112

[16] Kolathayar, S., Ghosh, P. 2011. Seismic active earth pressure on walls with bilinear backface using pseudo-dynamic approach. Geotechnical and Geological Engineering 29(3), 307-317. DOI: 10.1016/j.compgeo.2009.05.015

[17] Zhou, Y., Chen, F., Wang, X. 2018. Seismic active earth pressure for inclined rigid retaining walls considering rotation of the principal stresses with pseudo-dynamic method. International Journal of Geomechanics 18(7). DOI: 10.1061/(ASCE)GM.1943-5622.0001198

[18] Azad, A., Yasrobi, S.S., Pak, A. 2008. Seismic active pressure distribution history behind rigid retaining walls. Soil Dynamics and Earthquake Engineering 28(5), 365-375. DOI: 10.1016/j.soildyn.2007.07.003

[19] Shamsabadi, A., Xu, S.Y., Taciroglu, E. 2013. A generalized log-spiral-rankine limit equilibrium model for seismic earth pressure analysis. Soil Dynamics and Earthquake Engineering 49(6), 197-209. DOI: 10.1016/j.soildyn.2013.02.020

[20] Chen, J., Yang, Z., Hu, R., Zhang, H. 2016. Study on the seismic active earth pressure by variational limit equilibrium method. Shock and Vibration 2016(3), 1-10. DOI: 10.1155/2016/4158785

[21] Zhou, Q.Y., Zhou, Y.T., Wang, X.M., Yang, P.Z. 2017. Estimation of active earth pressure on a translating rigid retaining wall considering soil arching effect. Indian Geotechnical Journal. DOI: 10.1007/s40098-017-0252-8

[22] Zhou, Y., Chen, Q., Chen, F., Xue, X., & Basack, S. 2018. Active earth pressure on translating rigid retaining structures considering soil arching effect. European Journal of Environmental and Civil Engineering, 22(8), 910-926. DOI: 10.1080/19648189.2016.1229225

[23] Handy, R.L. 1985. The arch in soil arching. Journal of Geotechnical Engineering 111, 302–318. DOI:10.1061/(asce)0733-9410(1985)111:3(302)

[24] Paik, K.H., Salgado, R. 2003. Estimation of active earth pressure against rigid retaining walls considering arching effects. Geotechnique 53(7), 643-653.

[25] Goel, S., Patra, N.R. 2008. Effect of arching on active earth pressures for rigid retaining walls considering translation mode. International Journal of Geomechanics 8(2), 123-133. DOI: 10.1061/(ASCE)1532-3641 (2008)8:2(123)

[26] Li, J.P., Wang, M. 2014. Simplified method for calculating active earth pressure on rigid retaining walls considering the arching effect under translational mode. International Journal of Geomechanics 14(2), 282-290. DOI: 10.1061/(ASCE)GM.1943-5622. 0000313

[27] Li, D., Wang, W., Zhang, Q. 2014. Lateral earth pressure behind walls rotating about base considering arching effects. Mathematical Problems in Engineering 2014, 1-7. Doi: 10.1155/2014/715891

[28] Harrop-Williams, K.O. 1989. Geostatic wall pressures. Journal of Geotechnical Engineering 115, 1321–1325. DOI:10.1061/(asce)0733-9410(1989)115:9(1321)

[29] Cai, Y., Chen, Q., Zhou, Y., Nimbalkar, S., Yu, J. 2016. Estimation of passive earth pressure against rigid retaining wall considering arching effect in cohesive-frictional backfill under translation mode. International Journal of Geomechanics

17(4), 1-11. DOI: 10.1061/(ASCE)GM.1943-5622.0000786

[30] Rao, P., Chen, Q., Zhou, Y., Nimbalkar, S., & Chiaro, G. 2016. Determination of active earth pressure on rigid retaining wall considering arching effect in cohesive backfill soil. International Journal of Geomechanics, 16(3), 1-9. doi: 10.1061/(ASCE)GM.1943-5622.0000589

[31] Dalvi, R.S., Pise, P. J. 2012. Analysis of arching in soil-passive state. Indian Geotechnical Journal 42(2), 106-112. DOI: 10.1007/s40098-012-0004-8

[32] Dalvi, R.S., Bhosale, S.S., Pise, P.J. 2005. Analysis for passive earth pressure-catenary arch in soil. Indian Geotechnical Journal 35 (4), 388–400.